
Distributed stochastic gradient MCMC for federated learning

Khaoula El Mekkaoui^{1†}, Diego Mesquita¹, Paul Blomstedt², Samuel Kaski^{1,3}
¹Aalto University ²F-Secure ³University of Manchester

Abstract

Stochastic gradient MCMC methods, such as stochastic gradient Langevin dynamics (SGLD), enable large-scale posterior inference by leveraging noisy but cheap gradient estimates. However, when federated data are non-IID, the variance of distributed gradient estimates is amplified compared to its centralized version, and delayed communication rounds lead chains to diverge from the target posterior. In this work, we introduce the concept of *conductive gradients*, zero-mean stochastic gradients that serve as a mechanism for sharing probabilistic information between data shards. We propose a novel stochastic gradient estimator that incorporates the conductive gradients, and we show that it improves convergence on federated data when compared to distributed SGLD (DSGLD). We evaluate, *conductive gradient DSGLD* (CG-DSGLD) on metric learning and deep MLPs tasks. Experiments show that it outperforms standard DSGLD for non-IID federated data.

1 Introduction

Gradient-based Markov Chain Monte Carlo (MCMC) methods for computing Bayesian posteriors have become increasingly popular in recent years. Exact gradient evaluations, however, can be prohibitive even for moderately large data sets. Following the success of using stochastic gradients in large-scale optimization problems, and inspired by Welling and Teh (2011), many gradient-based MCMC algorithms have been adapted to capitalize on the idea of using fast but noisy gradient evaluations computed on mini-batches

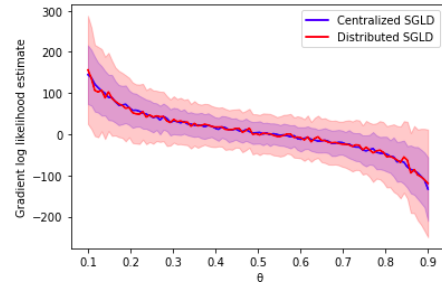


Figure 1: Comparison between gradient estimators using centralized (SGLD) and distributed data (DSGLD), for a model with Bernoulli likelihood and uniform prior. We computed gradients using 5 samples from a total of 30 observations generated from fair coin tosses. For DSGLD, we split data between 3 equally-available shards of same size but distinct means -0.1 , 0.5 and 0.9 . Error bars show one standard deviation. DSGLD has higher variance than SGLD even for this simple case.

of data (Ma *et al.*, 2015). Examples include stochastic gradient Langevin dynamics SGLD (Welling and Teh, 2011), stochastic gradient Hamiltonian Monte Carlo (SGHMC) (Chen *et al.*, 2014), and Riemann manifold Hamiltonian Monte Carlo (RMHMC) (Girolami and Calderhead, 2011). These methods have established themselves as popular choices for scalable MCMC sampling.

Complementary to data subsampling, which underlies the use of stochastic gradients, data can be partitioned across several workers and distributed computations can be used to scale up MCMC (Neiswanger *et al.*, 2014; Scott *et al.*, 2016; Terenin *et al.*, 2020; Wang *et al.*, 2015; Mesquita *et al.*, 2019). Federated learning would need the same methods, even though federated data are not actively distributed for computational profit, but instead they are at several independent clients or devices, and communication or privacy constraints may prevent data from being centralized into a server. In this work, we focus on stochastic gradient MCMC in federated settings and use distributed SGLD (DSGLD,

Ahn *et al.*, 2014) as our starting point.

While stochastic gradients provide an immediate reduction in computational cost, and thus better scaling properties, they may suffer from intrinsically high variance, leading to poor mixing rates and slow convergence (Dubey *et al.*, 2016). In distributed SG-MCMC settings, we need to choose mini-batches from the data subset held by an individual client, which amplifies the variance compared to choosing from all data in a centralized setting. This issue can be especially prominent if the data are highly heterogeneous, i.e., when distributed across clients in a non-IID manner. Figure 1 illustrates this phenomenon for a simple model with Bernoulli likelihood.

In this work, we propose a novel estimator for DSGLD for federated scenarios. As our method’s central mechanism, we define the notion of a *conductive gradient*, a zero-mean stochastic gradient constructed using independent approximations to the local likelihood factors. The role of the *conductive gradient* is to provide a global estimate of the target posterior which, when added to the unbiased gradient estimator proposed by Ahn *et al.* (2014), allows for information-sharing between clients. We call the resulting method *conductive gradient DSGLD* (CG-DSGLD). In practice, we have also observed that introducing these approximations is useful for delayed communication rounds, a known pathology of DSGLD. We also demonstrate empirically that CG-DSGLD outperforms DSGLD for non-IID federated data.

We provide convergence bounds for CG-DSGLD and use these results to gain insight about choosing adequate local likelihood approximations. We also provide an analysis for DSGLD, since no formal analysis appears to be available. In serial settings, an extensive effort has been conducted to provide technical analysis on the convergence of SGLD (Chen *et al.*, 2015; Nagapetyan *et al.*, 2017; Baker *et al.*, 2019; Teh *et al.*, 2016; Vollmer *et al.*, 2016), and due to its relatively straightforward formulation, we use it as a starting point for our analysis.

The remaining of the paper is organized as follows: In Section 2, we establish notation and provide a brief review of serial and distributed SGLD. In Section 3, we introduce the concept of conductive gradients and use it to construct a novel gradient estimator. In Section 4, we show convergence bounds for both DSGLD and CG-DSGLD. In Section 5, we show experimental results. Finally, we discuss related work in Section 6 and draw conclusions in Section 7.

2 Background and notation

Let $\mathbf{x} = \{x_1, \dots, x_N\}$ be a data set of size N and let $p(\theta|\mathbf{x}) \propto p(\theta) \prod_{i=1}^N p(x_i|\theta)$ be the density of a posterior distribution from which we wish to draw samples. Langevin dynamics (Neal, 2011) is a family of MCMC methods which utilizes the gradient of the log-posterior,

$$\nabla \log p(\theta|\mathbf{x}) = \nabla \log p(\theta) + \sum_{i=1}^N \nabla \log p(x_i|\theta),$$

to generate proposals in a Metropolis-Hastings sampling scheme. For large data sets, computing the gradient of the log-likelihood with respect to the entire data set \mathbf{x} becomes expensive. To mitigate this problem, stochastic gradient Langevin dynamics (SGLD) (Welling and Teh, 2011) uses stochastic gradients to approximate the full-data gradient.

Denoting by $\nabla \log p(\mathbf{x}^{(m)}|\theta_t) = \sum_{x \in \mathbf{x}^{(m)}} \nabla \log p(x|\theta_t)$ the gradient of the log-likelihood with respect to a mini-batch $\mathbf{x}^{(m)}$ of size m , SGLD draws samples from the target distribution using a stochastic gradient update of the form

$$\theta_{t+1} = \theta_t + \frac{h_t}{2} v(\theta_t) + \eta_t, \quad (1)$$

in which h_t is the step size, η_t is a noise variable sampled from $\mathcal{N}(0, h_t I)$ and where

$$v(\theta_t) = \nabla \log p(\theta_t) + \frac{N}{m} \nabla \log p(\mathbf{x}^{(m)}|\theta_t). \quad (2)$$

The step size is annealed according to a schedule satisfying $\sum_{t=1}^{\infty} h_t = \infty$ and $\sum_{t=1}^{\infty} h_t^2 < \infty$. Note that as $h_t \rightarrow 0$, the Metropolis-Hastings acceptance rate goes asymptotically to one and thus, the accept-reject step is typically ignored in SGLD. While a proper annealing schedule yields an asymptotically exact algorithm, constant step sizes are often used in practice.

2.1 DSGLD

In this paper, our focus is on SGLD in distributed settings (DSGLD), where we find data \mathbf{x} to be partitioned into S non-overlapping shards \mathbf{x}_s , each held by a client, such that $\mathbf{x} = \{\mathbf{x}_1, \dots, \mathbf{x}_S\}$. Equation (1) has been adapted to distributed settings (Ahn *et al.*, 2014). The main idea is that in each iteration, a mini-batch is sampled *within* a shard, say \mathbf{x}_s , and the shard itself is sampled by a scheduler with probability f_s , with $\sum_{s=1}^S f_s = 1$ and $f_s > 0$ for all s . This results in the update

$$\theta_{t+1} = \theta_t + \frac{h_t}{2} v_{s_t}(\theta_t) + \eta_t, \quad (3)$$

in which v is an unbiased gradient estimator given by

$$v_{s_t}(\theta_t) = \nabla \log p(\theta_t) + \frac{N_{s_t}}{f_{s_t} m} \nabla \log p(\mathbf{x}_{s_t}^{(m)}|\theta_t), \quad (4)$$

†corresponding author (khaoula.elmekkaoui@aalto.fi)

and where N_{s_t} denotes the size of shard \mathbf{x}_{s_t} , chosen at time t . Intuitively, if a mini-batch of m data points is chosen uniformly at random from \mathbf{x}_{s_t} , then N_{s_t}/m scales $\nabla \log p(\mathbf{x}_{s_t}^{(m)}|\theta_t)$ to be an unbiased estimator for $\nabla \log p(\mathbf{x}_{s_t}|\theta_t)$, while $f_{s_t}^{-1}$ further scales this gradient to be an unbiased estimator for $\nabla \log p(\mathbf{x}|\theta_t)$.

In order to reduce the overhead in workers communicating between each iteration, Ahn *et al.* (2014) further proposed a modified version, where multiple update steps within a shard are taken before moving to another worker, at the cost of some loss in asymptotic accuracy. It is worth noting that, while the data are distributed across multiple workers, the above sampling procedure may still be understood as being entirely serial. In practice, however, distributed settings are naturally amenable to running multiple chains in parallel.

3 CG-DSGLD: Distributed inference using conducive gradients

In DSGLD, stochastic gradient updates are computed on mini-batches sampled within the data shard of a specific client, which adds bias to the updates and increases variance globally. This is especially significant if the shards are heterogeneous, i.e., non-IID, as then local likelihood contributions vastly differ between two devices. To counteract this, we would like to make the local updates benefit from other shards’ information, ideally without significantly increasing either computational cost or memory requirements. Our strategy for achieving this goal is to augment the local updates, in Equation 3, with an auxiliary gradient computed on a tractable surrogate for the full-data likelihood $p(\mathbf{x}|\theta)$.

We assume here that the surrogate, denoted as $q(\theta)$, factorizes over shards, such as $q(\theta) = \prod_s q_s(\theta)$, where each $q_s(\theta)$ is itself a surrogate for $p(\mathbf{x}_s|\theta)$, i.e. the likelihood w.r.t. an entire shard s . Given these surrogates, we define the *conductive gradient* w.r.t. shard s as

$$g_s(\theta) = \nabla \log q(\theta) - \frac{1}{f_s} \nabla \log q_s(\theta).$$

Using the conducive gradient g_s we define our novel update rule as

$$\theta_{t+1} = \theta_t + \frac{h_t}{2} \left(v_{s_t}(\theta_t) + g_{s_t}(\theta_t) \right) + \eta_t. \quad (5)$$

Algorithm 1 describes our method, conducive gradient DSGLD (CG-DSGLD).

Remark 1 (Controlling exploration). *Note that conducive gradients can alternatively be written as*

$$g_s(\theta) = \nabla \log \frac{q(\theta)}{q_s(\theta) f_s^{-1}}, \quad (6)$$

making it explicit that these terms encourage the exploration of regions in which we believe, based on the approximations q and q_s , the posterior density to be high but the density within shard s to be low. We can explicitly control the extent of this exploration by multiplying the conducive gradient by a constant $\alpha > 0$ to obtain the modified gradient estimator:

$$\frac{N_s}{f_s m} \nabla \log p(\mathbf{x}_s^{(m)}|\theta) + \alpha g_s(\theta). \quad (7)$$

3.1 Choice of surrogates q_1, \dots, q_S

The key idea in choosing q_s is to obtain an approximation of $p(\mathbf{x}_s|\theta)$ with a parametric form, and to choose the parametric form such that $\nabla \log q_s(\theta)$ computation is inexpensive. It is particularly beneficial if the gradient can be computed in a single gradient evaluation instead of iterating over all data, of size N_s , of said shard s . Exponential family distributions are particularly convenient for this purpose, as they are closed under product operations, enabling us to compute $\nabla \log q(\theta_t)$ in a single gradient evaluation, which keeps the additional cost of our method negligible even when $S \gg m$.

In this work, we use a simulation-based approach to compute q_s by first drawing from $p_s \propto p(\mathbf{x}_s|\theta)$ locally employing SGLD, and using the resulting samples to compute the parameters of an exponential family approximation. To avoid communication overhead, q_1, \dots, q_S can be computed independently in parallel for each of the data shards and then communicated to the coordinating server once, before the CG-DSGLD steps take place.

4 Analysis

In this Section, we analyze the convergence of both DSGLD and the proposed CG-DSGLD. Besides reflecting the impact of heterogeneity among data shards, our bounds for CG-DSGLD also provide deeper insight on our strategy for choosing the surrogates q_1, \dots, q_S . We provide proofs in the supplementary material.

4.1 Convergence of DSGLD

We begin by analyzing the convergence of DSGLD under the same framework used for the analysis of SGLD by (Chen *et al.*, 2015) and subsequently adopted by (Dubey *et al.*, 2016), who directly tie convergence bounds to the variance of the gradient estimators. Besides certain regularity conditions adopted in these works, which we outline in the supplementary material, we make the following assumption:

Assumption 1. *The gradient of the log-likelihood of individual elements within each shard is bounded, i.e.,*

Algorithm 1 CG-DSGLD

Client-side $Update(T, \theta_0, s)$

Given: Total number of iterations T , step sizes $\{h_t\}_{t=0}^{T-1}$, initial chain state θ_0 , client number s .
for $t = 0 \dots T - 1$ **do**

Sample a mini-batch $\mathbf{x}_s^{(m)}$ of size m from \mathbf{x}_s
 $d_s \leftarrow \nabla \log p(\theta) + \frac{1}{f_s} \frac{N_s}{m} \nabla \log p(\mathbf{x}_s^{(m)} | \theta)$
▷ DSGLD estimator

$g_s \leftarrow -\frac{1}{f_s} \nabla \log q_s(\theta) + \nabla \log q(\theta)$
▷ Conducive gradient

$\theta_{t+1} \leftarrow \theta_t + \frac{h_t}{2} (d_s + g_s) + \eta_t$
▷ According to Eq. (5)

end for

Reassign_chain($\theta_0, \dots, \theta_T$)
▷ Send chain to server

Server-side Reassign_chain($\theta_0, \dots, \theta_T$)

Given: Client probabilities f_1, \dots, f_S .

Store the received chain

$c \sim \text{Categorical}(f_1, \dots, f_S)$
▷ Choose a client at random.

$Update(T, \theta_T, c)$
▷ Pass on chain to client c .

$\|\nabla \log p(x_i | \theta)\| \leq \gamma_s$, for all θ and $x_i \in \mathbf{x}_s$, and each $s \in \{1, \dots, S\}$.

We then proceed to derive the following bound on the convergence in mean squared error (MSE) of the Monte Carlo expectation $\hat{\phi} = T^{-1} \sum_{t=1}^T \phi(\theta_t)$ of a test function ϕ with respect to its expected value $\bar{\phi} = \int \phi(\theta) p(\theta | \mathbf{x}) d\theta$.

Theorem 1. *Let $h_t = h$ for all $t \in \{1, \dots, T\}$. Under standard regularity conditions and Assumption 1, the MSE of DSGLD for a smooth test function ϕ at time $K = hT$ is bounded, for some constant C independent of T and h , in the following manner:*

$$\mathbb{E} \left(\hat{\phi} - \bar{\phi} \right)^2 \leq C \left(\frac{\sum_s \frac{N_s^2}{f_s} \gamma_s^2}{mT} + \frac{1}{hT} + h^2 \right).$$

The bound in Theorem 1 depends explicitly on the ratio between squared shard sizes and their selection probabilities. This follows the intuition that both shard sizes and their availability play a role in the convergence speed of DSGLD.

Remark 2 (SGLD as a special case). *Note also that bound for DSGLD generalizes previous results for SGLD (Dubey et al., 2016). More specifically, if we*

combine all shards into a single data set $\mathbf{x} = \cup_s \mathbf{x}_s$ and let $\gamma \geq \gamma_1, \dots, \gamma_s$, we recover the bound for SGLD:

$$\mathbb{E} \left(\hat{\phi} - \bar{\phi} \right)^2 \leq C \left(\frac{N^2 \gamma^2}{mT} + \frac{1}{hT} + h^2 \right).$$

4.2 Convergence of CG-DSGLD

The following result states that when $g_s(\theta)$ is added to the stochastic gradient in a DSGLD setting, the resulting estimator remains a valid estimator for the gradient of the full-data log-likelihood.

Lemma 1. *Assume $\log q_1, \dots, \log q_S$ are Lipschitz continuous. Given a data set \mathbf{x} partitioned into shards $\mathbf{x}_1, \dots, \mathbf{x}_S$, with respective sample sizes N_1, \dots, N_S and shard selection probabilities f_1, \dots, f_S , the following gradient estimator,*

$$\frac{N_s}{f_s m} \nabla \log p(\mathbf{x}_s^{(m)} | \theta) + g_s(\theta),$$

is an unbiased estimator of $\nabla \log p(\mathbf{x} | \theta)$ with finite variance.

With the validity of our estimator established, we now provide the convergence bound for CG-DSLGD, stated in Theorem 2.

Lemma 2. *If $\log q_1, \dots, \log q_S$ are everywhere differentiable and Lipschitz continuous, then the average value of $\|\nabla \log p(x_i | \theta) - N_s^{-1} \nabla \log q_s(\theta)\|^2$, taken over $x_i \in \mathbf{x}_s$, is bounded by some ϵ_s^2 , for each θ .*

Theorem 2. *Let $h_t = h$ for all $t \in \{1, \dots, T\}$. Assume $\log q_1, \dots, \log q_S$ are Lipschitz continuous. Under standard regularity conditions and Assumption 1, the MSE of CG-DSGLD (defined in Algorithm 1) for a smooth test function ϕ at time $K = hT$ is bounded, for some constant C independent of T and h in the following manner:*

$$\mathbb{E} \left(\hat{\phi} - \bar{\phi} \right)^2 \leq C \left(\frac{1}{mT} \sum_s \frac{N_s^2}{f_s} \epsilon_s^2 + \frac{1}{hT} + h^2 \right).$$

In other words, Theorem 2 tells us that we can counteract the effect of data heterogeneity by choosing surrogates q_s 's that make the constants ϵ_s^2 's as small as possible.

Remark 3 (Revisiting the choice of q_s 's). *Naturally, the choice of q_s exerts direct influence on ϵ_s^2 . Doing so analytically is difficult, but we can get further insight if we choose q_s that achieves*

$$\min_{q_s} \max_{\theta} \|\nabla \log p(\mathbf{x}_s | \theta) - \nabla \log q_s(\theta)\|^2, \quad (8)$$

which itself minimizes an upper-bound for ϵ_s^2 . Note that Equation 8 reaches its minimum when $q_s(\theta)$ is equal

to $p(\mathbf{x}_s|\theta)$. Therefore, it is sensible to choose q_s that approximates the local likelihood contributions as well as possible, as previously described in Subsection 3.1. We provide further details about the upper-bound in the supplementary material.

5 Experiments

In this Section, we demonstrate the performance of CG-DSGLD for increasingly complex models under the non-IID data regime, which is a defining characteristic of federated settings.

In Subsection 5.1, we provide a visual illustration of a pathology that afflicts DSGLD when the number of updates within the same client increases, and which is easily circumvented by our method. In Subsection 5.2, we consider the task of inferring Bayesian metric learning posteriors from highly non-IID data. Finally, in Subsection 5.3, we show how our method can be employed to learn Bayesian neural networks in a distributed fashion, and analyze how its behavior changes as the amount of heterogeneity between shards increases, when compared to its original counterpart.

While these models are progressively more complex, we highlight that, using multivariate Gaussians as the approximations q_1, \dots, q_S to each within-shard likelihood function, we were still able to obtain good and computationally scalable results for CG-DSGLD. For the first set of experiments, we derive analytic forms for the approximations q_s , which is possible due to the simplicity of the target model. For the remaining ones, we employ SGLD independently for $s = 1, \dots, S$ and use the samples obtained to compute the mean vector and covariance matrix that parameterize q_s . All experiments were implemented using PyTorch¹.

5.1 Heterogeneous shards and delayed communication

An ideal sampling scheme would, in theory, update the chain once at a device and immediately pass it over to another device in the next iteration. However, such a short communication cycle would result in a large overhead and is unrealistic in federated settings. To ameliorate the problem, Ahn *et al.* (2014) proposed making a number of chain updates before moving to another device. However, the authors reported that as the number of iterations within each client and shard increases, the algorithm tends to lose sample efficiency and effectively sample from a mixture of local posteriors, $\frac{1}{S} \sum_{s=1}^S p(\theta|\mathbf{x}_s)$, instead of the true posterior. With heterogeneous data shards, the effect is particularly noticeable. In this experiment, we illustrate the

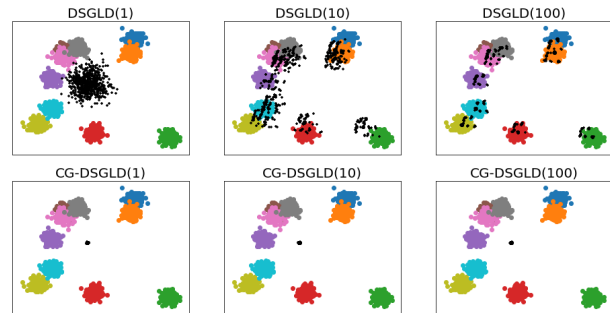


Figure 2: Posterior samples of the global mean (black) in DSGLD and CG-DSGLD, as a function of the number of shard-local updates (shown in parentheses in each title). The colored dots are the data samples, different shards having different color. CG-DSGLD converges to the target posterior in all cases, while DSGLD approaches a mixture of local posteriors as the number of local updates increases.

pathology and show how CG-DSGLD overcomes it.

Model: We consider inference for the mean vector μ of normally distributed data under the simple model

$$p(\mu|\mathbf{x}) \propto \mathcal{N}(\mu|\mathbf{0}, I) \prod_{s=1}^S \mathcal{N}(\mathbf{x}_s|\mu, I). \quad (9)$$

Setting: We generate $S = 10$ disjoint data subsets $\mathbf{x}_1, \dots, \mathbf{x}_S$ of size 200, each respectively from $\mathcal{N}(\mu_1, I)$ with μ_1 uniformly sampled from the $[-6, 6] \times [-6, 6]$ square (the colored dots in Fig 2). We then perform inference on the overall mean μ using the model (9). We sample the same number of posterior samples using both DSGLD and CG-DSGLD with fixed step-size $h = 10^{-4}$, mini-batch size $m = 10$ and $f_1 = \dots = f_S = 1/S$. The first 20000 samples were discarded as burn-in, and the remaining ones were thinned by 100. We use a single Gaussian approximation $q_s(\theta) = \mathcal{N}(\theta|\bar{\mathbf{x}}_s, N^{-1}I)$, for each $s = 1 \dots S$.

Results: Figure 2 shows the posterior samples as a function of the number of local updates the method takes before passing the chain to the next device. For comparison, Figure 3a shows samples from the analytical posterior. As we can see from the results, the proposed method (CG-DSGLD) converges adequately to the true posterior while DSGLD diverges towards a mixture of local approximations. This discrepancy becomes more prominent as we further increase the number of local updates, therefore delaying communication. Figure 3b compares the convergence in terms of the number of posterior samples. While DSGLD with a hundred local updates converges as fast as CG-DSGLD,

¹<https://pytorch.org>

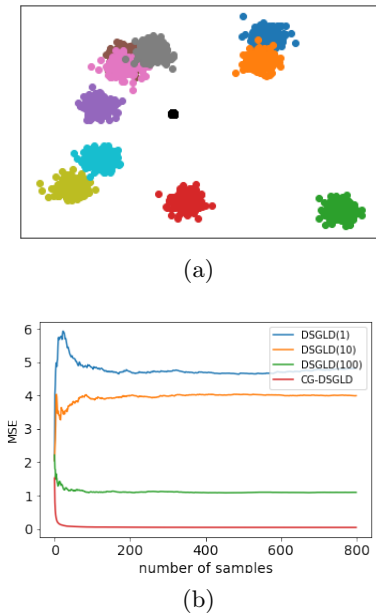


Figure 3: (a) Samples from the analytical posterior, for comparison with Figure 1. (b) Quantitative comparison of MSE $|\bar{\mu} - \hat{\mu}|^2$ in estimating the global mean, as a function of the number of posterior samples, showing CG-DSGLD clearly outperforms DSGLD. Numbers in parentheses indicate number of successive local shard updates; for CG-DSGLD the curves are almost identical, independently of the number, and only one is shown. Only CG-DSGLD converges to $\bar{\mu}$.

it plateaus at a higher MSE. Note that in contrast with DSGLD, CG-DSGLD is insensitive to the number of local updates in the current experiment.

Quantifying ϵ_s^2 's. Theorem 2 states that the upper-bound on the MSE of CG-DSGLD deteriorate as $\epsilon_1^2, \dots, \epsilon_S^2$ increase. While computing ϵ_s^2 's is intractable for most models, we can approximate it in this simple case using a grid. The same can be done for γ_s^2 's, which govern the DSGLD bound in similar manner. Figure 4 shows that $\epsilon_s^2 \ll \gamma_s^2$ for all shards s . This phenomenon also corroborate with the results in Figure 3b, which show the MSE of CG-DSLGD converges to much smaller values than DSGLD.

5.2 Metric learning

Given sets of similar \mathcal{S} and dissimilar \mathcal{D} pairs of vectors from $\mathcal{X} = \{x_n\}_{n=1}^N \in \mathbb{R}^D$, metric learning concerns the task of learning a distance metric matrix $A \in \mathbb{R}^{D \times D}$ such that the Mahalanobis distance

$$\|x_i - x_j\|_A = \sqrt{(x_i - x_j)^\top A (x_i - x_j)}$$

is low if $(x_i, x_j) \in \mathcal{S}$ and high if $(x_i, x_j) \in \mathcal{D}$.

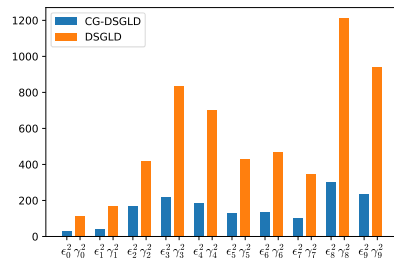


Figure 4: The constants ϵ_s^2 's, which govern CG-DSGLDour method, are much smaller than γ_s^2 's from DSGLD, resulting in tighter bounds. The barplots shows grid-based approximations these for these values in the mean estimation model.values for the 5.1

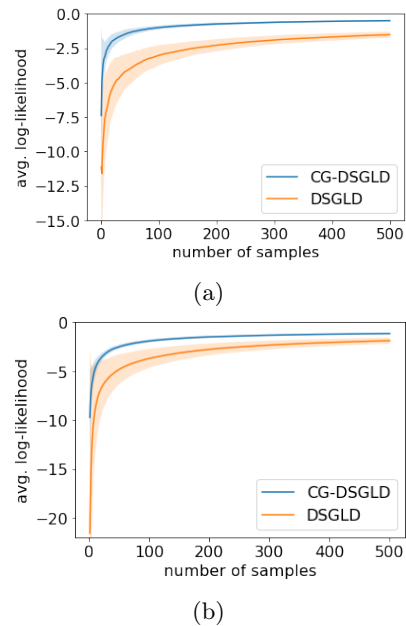


Figure 5: **Metric learning.** Average log-likelihood values as a function of the number of samples for both DSGLD and CG-DSGLD, measured on (a) learning data and (b) on a held-out set of test samples. The curves show the mean and standard deviation (error bars) for ten repetitions of the experiment, with different random seeds. CG-DSGLD converges faster and to better predictions than DSGLD, both for training data and for test data.

Model: We consider inference on the Bayesian metric learning model proposed by Yang *et al.* (2007), in which it is assumed that A can be expressed as $\sum_k \gamma_k \mathbf{v}_k \mathbf{v}_k^\top$ where $\mathbf{v}_1, \dots, \mathbf{v}_K$ are the top K eigenvectors of $X = [x_1^\top, \dots, x_N^\top]$. The likelihood function for each pair (x_i, x_j) from \mathcal{S} or \mathcal{D} is given by

$$y_{ij} | (x_i, x_j), A, \mu \sim \text{Ber} \left(\frac{1}{1 + \exp(y_{ij} (\|x_i - x_j\|_A^2 - \mu))} \right)$$

where y_{ij} equals one if $(x_i, x_j) \in \mathcal{S}$ and equals zero, if $(x_i, x_j) \in \mathcal{D}$. While having $\gamma = [\gamma_1, \dots, \gamma_K] \succ 0$ is enough to guarantee that A is a distance metric, this is further relaxed and a diagonal Gaussian prior is put on γ .

Setting: We have devised a data set for metric learning based on the Spoken Letter Recognition² (isolet) data, which encompasses 7797 examples split among 26 classes. We have created $|\mathcal{S}| = 5000$ and $|\mathcal{D}| = 5000$ pairs of similar and dissimilar vectors, respectively, using the labels of the isolet examples, i.e., samples are considered similar if they belong to the same class and dissimilar otherwise. We split these pairs into $S = 10$ data shards of identical size, in a manner that there is no overlap in the classes used to create the sets of pairs \mathcal{S}_s and \mathcal{D}_s in each shard $s = 1 \dots S$. Additionally, we created another thousand pairs of equally split similar and dissimilar examples that we held out for the test.

We set $f_1 = \dots = f_S = \frac{1}{S}$ and run both DSGLD and CG-DSGLD with constant step size 10^{-3} and mini-batch size $m = 256$. We use simple Gaussian approximations for q_1, \dots, q_S , with mean and covariance parameters computed numerically using three thousand samples from

$$\prod_{(x_i, x_j) \in \mathcal{S}_s \cup \mathcal{D}_s} \text{Ber} \left(y_i \left| \frac{1}{1 + \exp(y_{ij} (\|x_i - x_j\|_A^2 - \mu))} \right. \right),$$

obtained running SGLD independently for each client. It is worth highlight that these approximations are only computed once at the beginning of training, and then communicated to the server.

Results: Figure 5 shows results in terms of average log-likelihood as a function of the number of samples. The results show that *i*) CG-DSGLD achieves better performance than DSGLD both in learning and on test data; and *ii*) CG-DSGLD is more communication-efficient than DSGLD, i.e., it converges faster. Furthermore, CG-DSGLD exhibits overall lower standard deviation.

5.3 Bayesian neural networks

We now gauge the performance of the proposed CG-DSGLD for posterior inference on a deep Multi-Layer Perceptron (MLP) both for federated IID and for federated non-IID data.

Model: We consider an MLP with three hidden layers. The first two hidden layers consist of 18 nodes each, and the last one of 8. We equip all hidden nodes with the rectified linear unit (ReLU) activation function, and we apply the Softmax function to the output of the network. Since we employ this network for a classification task, we use the cross-entropy loss function.

Setting: For this experiment, we create a series of $S = 30$ label-imbalanced data shards based on the SUSY³ dataset. For the IID case, we draw the proportions π_1, \dots, π_S of positive samples in each shard $s = 1, \dots, S$ from a symmetric Beta distribution with parameters $a = b = 100$. In this case, each data shard is approximately balanced. For the non-IID case, we sample the proportions from a Beta with both parameters equal to 0.5 instead. When $a = b = 0.5$, half of the shards tend to have mostly positive and the other half tends to have mostly negative labels, enforcing diversity between shards.

All the shards mentioned above comprise 9×10^4 samples, and we hold out an additional balanced shard for evaluation. We ran CG-DSGLD and DSGLD, with even shard selection probabilities, for 5×10^3 rounds of communication, between which 40 shard-local updates take place. For both methods, we adopt fixed step-size $h = 10^{-4}$ and use mini-batches of size $m = 50$. The first 2×10^4 samples were discarded for each method, and the remaining ones were thinned by two. Similarly to the previous experiment, we computed the conducive terms by drawing independently from densities proportional to the local likelihoods and imposing diagonal-multivariate normal approximations based on these samples.

Results: Table 1 shows results in terms of average log-likelihood, evaluated on test and train data. For the non-IID case, CG-DSGLD significantly outperforms DSGLD on the test set. It is worth noting the low average log-likelihood achieved by DSGLD during training is a clear sign that it converged to models that do not generalize well. For the IID case, both methods perform similarly. In both cases, CG-DSGLD shows a steep decrease in variance.

Table 1: **MLPs.** Average log-likelihood for MLPs learned with DSGLD and CG-DSGLD. For the non-IID case, CG-DSGLD clearly learns better models. For the IID case, both methods show similar performance. Results reflect the outcome of ten repetitions (mean \pm standard deviation). For all cases, CG-DSGLD results in smaller standard deviation.

		Homogenous (IID)	Heterogenous (non-IID)
DSGLD	train	-0.69 \pm 0.001	-0.44 \pm 0.062
	test	-0.70 \pm 0.001	-1.11 \pm 0.312
CG-DSGLD	train	-0.69 \pm 0.00022	-0.67 \pm 0.03
	test	-0.69 \pm 0.00022	-0.67 \pm 0.03

²<https://archive.ics.uci.edu/ml/datasets/isolet>

³<https://archive.ics.uci.edu/ml/datasets/SUSY>

6 Related work

Variance reduction for stochastic optimization.

Variance reduction has been previously explored to improve the convergence of stochastic gradient descent (e.g. Johnson and Zhang, 2013; Defazio *et al.*, 2014a,b). While federated optimization has gained increasing attention (Konecný *et al.*, 2016), variance reduction for distributed stochastic gradient descent has received only limited attention (De and Goldstein, 2016; Li *et al.*, 2020) so far.

Variance reduction for serial SG-MCMC. To the best of our knowledge, this is the first work proposing a variance reduction scheme for DSGLD. Previous works by Dubey *et al.* (2016); Baker *et al.* (2019) have proposed strategies to alleviate the effect of high variance in SGLD, for serial settings. Dubey *et al.* (2016) proposed two algorithms, SAGA-LD and SVRG-LD, both of which are based on using previously evaluated gradients to approximate gradients for data points not visited in a given iteration. The first algorithm, SAGA-LD, requires a record of individual gradients for each data point to be maintained. In the second one, SVRG-LD, the gradient on the entire data set needs to be periodically evaluated. The recently proposed SGLD-CV Baker *et al.* (2019) uses posterior mode estimates to build control variates, which are added to the gradient estimates to speed up convergence. Like SGLD-CV, our algorithm can be seen as a control variate method (Ripley, 1987), but designed for distributed settings.

7 Conclusion

We proposed CG-DSGLD, a novel method that incorporates computationally feasible approximations of each device’s local likelihood contribution to improve the convergence of distributed SGLD for federated data. Experiments showed that our method outperforms DSGLD for federated scenarios. Our method can be seen as a variance reduction strategy for DSGLD. To the best of our knowledge, this is the first treatment of SG-MCMC for federated settings.

We analyzed the convergence of DSGLD to understand the influence of both data heterogeneity and device availability. We also showed convergence bounds for CG-DSGLD and discussed how it supports our choice of local likelihood surrogates.

Furthermore, given suitable surrogates q_1, \dots, q_S , such as exponential family approximations, CG-DSGLD can be simultaneously made efficient both in terms of memory and computation, imposing no significant overhead compared to DSGLD. Nonetheless, we leave open the possibility of employing more expressive or computationally cheaper surrogates $\{q_s\}_{s=1}^S$, such as

non-parametric methods or variational approximations, respectively.

References

- Ahn, S., Shahbaba, B., and Welling, M. (2014). Distributed stochastic gradient MCMC. In *International Conference on Machine Learning (ICML)*.
- Baker, J., Fearnhead, P., Fox, E. B., and Nemeth, C. (2019). Control variates for stochastic gradient MCMC. *Statistics and Computing*, **29**(3), 599–615.
- Chen, C., Ding, N., and Carin, L. (2015). On the convergence of stochastic gradient MCMC algorithms with high-order integrators. In *Advances in Neural Information Processing Systems (NeurIPS)*.
- Chen, T., Fox, E. B., and Guestrin, C. (2014). Stochastic gradient Hamiltonian Monte Carlo. In *International Conference on Machine Learning (ICML)*.
- De, S. and Goldstein, T. (2016). Efficient distributed sgd with variance reduction. In *International Conference on Data Mining (ICDM)*.
- Defazio, A., Domke, J., and Caetano (2014a). Finito: A faster, permutable incremental gradient method for big data problems. In *International Conference on Machine Learning (ICML)*.
- Defazio, A., Bach, F., and Lacoste-Julien, S. (2014b). Saga: A fast incremental gradient method with support for non-strongly convex composite objectives. In *Advances in Neural Information Processing Systems (NeurIPS)*.
- Dubey, K. A., Reddi, S. J., Williamson, S. A., Póczos, B., Smola, A. J., and Xing, E. P. (2016). Variance reduction in stochastic gradient langevin dynamics. In *Advances in Neural Information Processing Systems (NeurIPS)*.
- Girolami, M. and Calderhead, B. (2011). Riemann manifold langevin and hamiltonian monte carlo methods. *Journal of the Royal Statistical Society: Series B (Statistical Methodology)*, **73**(2), 123–214.
- Johnson, R. and Zhang, T. (2013). Accelerating stochastic gradient descent using predictive variance reduction. In *Advances in Neural Information Processing Systems (NeurIPS)*.
- Konecný, J., McMahan, H. B., Ramage, D., and Richtárik, P. (2016). Federated optimization: Distributed machine learning for on-device intelligence. *ArXiv e-print*.
- Li, B., Cen, S., Chen, Y., and Chi, Y. (2020). Communication-efficient distributed optimization in networks with gradient tracking and variance reduction. In *Artificial Intelligence and Statistics (AISTATS)*.

- Ma, Y.-A., Chen, T., and Fox, E. (2015). A complete recipe for stochastic gradient MCMC. In *Advances in Neural Information Processing Systems (NeurIPS)*.
- Mesquita, D., Blomstedt, P., and Kaski, S. (2019). Embarrassingly parallel MCMC using deep invertible transformations. In *Uncertainty in Artificial Intelligence (UAI)*.
- Nagapetyan, T., Duncan, A. B., Hasenclever, L., Vollmer, S. J., Szpruch, L., and Zygalkakis, K. (2017). The true cost of stochastic gradient Langevin dynamics. *ArXiv e-print*.
- Neal, R. (2011). MCMC using Hamiltonian dynamics. In S. Brooks, A. Gelman, G. Jones, and X.-L. Meng, editors, *Handbook of Markov Chain Monte Carlo*. Chapman and Hall/CRC, New York.
- Neiswanger, W., Wang, C., and Xing, E. P. (2014). Asymptotically exact, embarrassingly parallel MCMC. In *Uncertainty in Artificial Intelligence (UAI)*.
- Ripley, B. D. (1987). *Stochastic Simulation*. John Wiley & Sons, Inc., USA.
- Scott, S. L., Blocker, A. W., Bonassi, F. V., Chipman, H. A., George, E. I., and McCulloch, R. E. (2016). Bayes and big data: The consensus Monte Carlo algorithm. *International Journal of Management Science and Engineering Management*, **11**(2), 78–88.
- Teh, Y. W., Thiery, A. H., and Vollmer, S. J. (2016). Consistency and fluctuations for stochastic gradient Langevin dynamics. *Journal of Machine Learning Research*, **17**(1), 193–225.
- Terenin, A., Simpson, D., and Draper, D. (2020). Asynchronous gibbs sampling. In *Artificial Intelligence and Statistics (AISTATS)*.
- Vollmer, S. J., Zygalkakis, K. C., and Teh, Y. W. (2016). Exploration of the (non-) asymptotic bias and variance of stochastic gradient Langevin dynamics. *Journal of Machine Learning Research*, **17**(1), 5504–5548.
- Wang, X., Guo, F., Heller, K. A., and Dunson, D. B. (2015). Parallelizing MCMC with random partition trees. In *Advances in Neural Information Processing Systems (NeurIPS)*.
- Welling, M. and Teh, Y. W. (2011). Bayesian learning via stochastic gradient Langevin dynamics. In *International Conference on Machine Learning (ICML)*.
- Yang, L., Jin, R., and Sukthankar, R. (2007). Bayesian active distance metric learning. *Uncertainty in Artificial Intelligence (UAI)*.

A Background on convergence analysis for SGLD

Let ψ be the functional that solves the Poisson equation $\mathcal{L}\psi = \phi - \hat{\phi}$. Assume ψ is bounded up to its third order derivative by a function Γ , such that $\|\mathcal{D}^k\psi\| \leq C_k\Gamma^{p_k}$ with $C_k, p_k > 0 \forall k \in \{0, \dots, 3\}$ with \mathcal{D}^k denoting the k th order derivative. Assume as well that the expectation of Γ w.r.t. θ_t is bounded ($\sup_t \mathbb{E}\Gamma^p[\theta_t] \leq \infty$) and that Γ is smooth such that $\sup_{s \in (0,1)} \Gamma^p(s\theta + (1-s)\theta') \leq C(\Gamma^p(\theta) + \Gamma^p(\theta'))$, $\forall \theta, \theta', p \leq \max_k 2p_k$, for some $C > 0$. Under these regularity conditions, Chen *et al.* (2015) showed the following result.

Theorem 3 (See Chen *et al.* (2015)). *Let U_t be an unbiased estimate of U , the unnormalized negative log posterior, and $h_t = h$ for all $t \in \{1, \dots, T\}$. Let $\Delta V_t = (\nabla U_t - \nabla U) \cdot \nabla$. Under the assumptions above, for a smooth test function ϕ , the MSE OF SGLD at time $K = hT$ is bounded for some $C > 0$ independent of (T, h) as:*

$$\mathbb{E}[(\bar{\phi} - \hat{\phi})^2] \leq C \left(\frac{\frac{1}{T} \sum_t \mathbb{E}[\|\Delta V_t\|^2]}{T} + \frac{1}{Th} + h^2 \right) \quad (1a)$$

Equation (1a) can also be written as:

$$\mathbb{E}[(\bar{\phi} - \hat{\phi})^2] \leq C \left(\frac{\frac{1}{T} \sum_t \mathbb{E}[\|\Delta V_t \psi(\theta_t)\|^2]}{T} + \frac{1}{Th} + h^2 \right). \quad (2a)$$

For further analysis we add the assumption that $(\Delta V_t \psi(\theta))^2 \leq C' \|\nabla U_t(\theta) - \nabla U(\theta)\|^2$ for some $C' > 0$.

B Proof of Theorem 1: Convergence of DSGLD

Here, we follow the footprints of Chen *et al.* (2015) later adopted by Dubey *et al.* (2016). Thus, we focus on bounding $\frac{1}{T} \sum_t \mathbb{E}[(\Delta V_t \psi(\theta_t))^2]$, when $U_t(\theta_t) = v_{s_t}(\theta_t)$. For some $C' > 0$, we have:

$$\frac{1}{C'T} \sum_t \mathbb{E}[(\Delta V_t \psi(\theta_t))^2] \leq \frac{1}{T} \sum_t \mathbb{E}[\|\nabla U_t(\theta_t) - \nabla U(\theta_t)\|^2] \quad (3a)$$

$$= \frac{1}{T} \sum_t \mathbb{E} \left[\left\| \frac{1}{f_s} \frac{N_s}{m} \nabla \log p(\mathbf{x}_{s_t}^{(m)} | \theta_t) - \nabla \log p(\mathbf{x} | \theta_t) \right\|^2 \right] \quad (3b)$$

$$= \frac{1}{Tm^2} \sum_t \mathbb{E} \left[\left\| \sum_{x_i \in \mathbf{x}_{s_t}^{(m)}} \frac{1}{f_s} N_s \nabla \log p(x_i | \theta_t) - \nabla \log p(\mathbf{x} | \theta_t) \right\|^2 \right] \quad (3c)$$

$$= \frac{1}{m^2} \mathbb{E}_s \mathbb{E}_{\mathbf{x}_{s_t}^{(m)} | s_t} \left[\left\| \sum_{x_i \in \mathbf{x}_{s_t}^{(m)}} \frac{1}{f_s} N_s \nabla \log p(x_i | \theta_t) - \nabla \log p(\mathbf{x} | \theta_t) \right\|^2 \right] \quad (3d)$$

$$\leq \frac{1}{m^2} \mathbb{E}_s \left[\mathbb{E}_{\mathbf{x}_{s_t}^{(m)} | s_t} \left[\sum_{x_i \in \mathbf{x}_{s_t}^{(m)}} \left\| \frac{1}{f_s} N_s \nabla \log p(x_i | \theta_t) \right\|^2 \right] \right] \quad (3e)$$

$$= \frac{1}{m^2} \mathbb{E}_s \left[m \frac{N_s^2}{f_s^2} \mathbb{E}_{x_i | s_t} \left[\left\| \nabla \log p(x_i | \theta_t) \right\|^2 \right] \right] \quad (3f)$$

$$\leq \frac{1}{m} \mathbb{E}_s \left[\frac{N_s^2}{f_s^2} \gamma_s^2 \right] = \frac{1}{m} \sum_s f_s \frac{N_s^2}{f_s^2} \gamma_s^2 = \frac{1}{m} \sum_s \frac{N_s^2}{f_s} \gamma_s^2 \quad (3g)$$

Here, $\mathbb{E}_{\mathbf{x}_{s_t}^{(m)} | s_t}$ denotes that the expectation is taken w.r.t. a mini-batch of size m with elements drawn with replacement and equal probability from shard s_t . Expectations without explicit subscripts are taken w.r.t. all random variables. To advance from Equation (3c) to (3d), we use law of iterated expectations and the fact that $\mathbb{E}[\|\sum_i r_i\|^2] = \sum_i \mathbb{E}[\|r_i\|^2]$ for zero-mean independent r_i 's. To advance from Equation (3d) to (3e), we use $\mathbb{E}[\|r - \mathbb{E}[r]\|^2] \leq \mathbb{E}[\|r\|^2]$. Substituting Equation (3g) in Equation (2a) yields the desired result.

C Proof of Lemma 1: Unbiasedness and finite variance

Recall that the for the DSGLD update (Ahn *et al.*, 2014) we have

$$\mathbb{E}_{s, \mathbf{x}_{s_t}^{(m)}} \left[\frac{1}{f_s} \frac{N_s}{m} \nabla \log p(\mathbf{x}_{s_t}^{(m)} | \theta_t) \right] = \nabla \log p(\mathbf{x} | \theta_t).$$

Furthermore, for *conductive gradients* we have that:

$$\mathbb{E}_s \left[\nabla q(\theta_t) - \frac{1}{f_s} \nabla q_s(\theta_t) \right] = q(\theta_t) - \sum_s f_s \frac{1}{f_s} q_s(\theta_t) = 0.$$

Since the CG-DSGLD estimator is the sum of the DSGLD estimator and the *conductive gradient*, it is unbiased.

The sufficient condition for the DSGLD estimator to have finite variance is that the unnormalized log posterior is Lipschitz continuous. Similarly, since q_1, \dots, q_S are also Lipschitz continuous, their first derivatives are bounded, so the conducive gradient is a convex combination of bounded functions and has finite variance. Thus, their sum, the CG-DSGLD estimator has finite variance.

D Proof of Theorem 2: Convergence of CG-DSGLD

We now bound $\frac{1}{T} \sum_t \mathbb{E}[(\Delta V_t \psi(\theta_t))^2]$ for the CG-DSGLD update equation, when $U_t(\theta_t) = v_{s_t}(\theta_t) + g_{s_t}(\theta_t)$.

$$\begin{aligned} & \frac{1}{C'T} \sum_t \mathbb{E}[(\Delta V_t \psi(\theta_t))^2] \\ & \leq \frac{1}{T} \sum_t \mathbb{E}[\|\nabla U_t(\theta_t) - \nabla U(\theta_t)\|^2] \end{aligned} \quad (4a)$$

$$= \frac{1}{Tm^2} \sum_t \mathbb{E} \left[\left\| \sum_{x_i \in \mathbf{x}_{s_t}^{(m)}} \frac{1}{f_s} (N_s \nabla \log p(x_i|\theta_t) - \nabla \log q_s(\theta_t)) + \nabla \log q(\theta_t) - \nabla \log p(\mathbf{x}|\theta_t) \right\|^2 \right] \quad (4b)$$

$$= \frac{1}{m^2} \mathbb{E}_s \mathbb{E}_{\mathbf{x}_{s_t}^{(m)} | s_t} \left[\left\| \sum_{x_i \in \mathbf{x}_{s_t}^{(m)}} \frac{1}{f_s} (N_s \nabla \log p(x_i|\theta_t) - \nabla \log q_s(\theta_t)) + \nabla \log q(\theta_t) - \nabla \log p(\mathbf{x}|\theta_t) \right\|^2 \right] \quad (4c)$$

$$\leq \frac{1}{m^2} \mathbb{E}_s \left[\mathbb{E}_{\mathbf{x}_{s_t}^{(m)} | s_t} \left[\left\| \sum_{x_i \in \mathbf{x}_{s_t}^{(m)}} \frac{1}{f_s} (N_s \nabla \log p(x_i|\theta_t) - \nabla \log q_s(\theta_t)) \right\|^2 \right] \right] \quad (4d)$$

$$= \frac{1}{m^2} \mathbb{E}_s \left[m \frac{N_s^2}{f_s^2} \mathbb{E}_{x_i | s_t} \left[\left\| \nabla \log p(x_i|\theta_t) - N_s^{-1} \nabla \log q_s(\theta_t) \right\|^2 \right] \right] \quad (4e)$$

$$= \frac{1}{m^2} \sum_s f_s m \frac{N_s^2}{f_s^2} \mathbb{E}_{x_i | s_t} \left[\left\| \nabla \log p(x_i|\theta_t) - N_s^{-1} \nabla \log q_s(\theta_t) \right\|^2 \right] \quad (4f)$$

$$\leq \frac{1}{m} \sum_s \frac{N_s^2}{f_s} \epsilon_s^2 \quad (4g)$$

We proceed from Equation (4b) to (4c) using the law of iterated expectations and the fact that $\mathbb{E}[\|\sum_i r_i\|^2] = \sum_i \mathbb{E}[\|r_i\|^2]$ for zero-mean independent r_i 's. To transition from Equation (4c) to (4d), we use $\mathbb{E}[\|r - \mathbb{E}[r]\|^2] \leq \mathbb{E}[\|r\|^2]$. The last line is obtained using *Lemma 2*. We use this bound and Equation 2a to get the desired result.

E More details on Remark 3

Following *Lemma 2* and assuming that ϵ_s^2 is a tight bound, i.e.

$$\epsilon_s^2 := \frac{1}{N_s} \sum_{x_i \in \mathbf{x}_s} \left\| \nabla \log p(x_i|\theta) - \frac{1}{N_s} \nabla \log q_s(\theta) \right\|^2, \quad (5a)$$

choosing q_s that minimizes ϵ_s^2 is equivalent to finding

$$\min_{q_s} \max_{\theta} \frac{1}{N_s} \sum_{x_i \in \mathbf{x}_s} \left\| \nabla \log p(x_i|\theta) - \frac{1}{N_s} \nabla \log q_s(\theta) \right\|^2, \quad (5b)$$

which is equal to

$$\frac{1}{N_s} \min_{q_s} \max_{\theta} \sum_{x_i \in \mathbf{x}_s} \left[\|\nabla \log p(x_i|\theta)\|^2 + \frac{1}{N_s^2} \|\nabla \log q_s(\theta)\|^2 - \frac{2}{N_s} (\nabla \log q_s(\theta))^\top \nabla \log p(x_i|\theta) \right], \quad (5c)$$

and can be further developed into

$$\frac{1}{N_s} \min_{q_s} \max_{\theta} \left[\sum_{x_i \in \mathbf{x}_s} \|\nabla \log p(x_i|\theta)\|^2 \right] + \frac{1}{N_s} \|\nabla \log q_s(\theta)\|^2 - \frac{2}{N_s} (\nabla \log q_s(\theta))^\top \nabla \log p(\mathbf{x}_s|\theta). \quad (5d)$$

Completing the squares and using $\max a + b \leq \max a + \max b$, we get the following upper-bound for Equation 5b:

$$\frac{1}{N_s^2} \min_{q_s} \max_{\theta} \left[\|\nabla \log q_s(\theta) - \nabla \log p(\mathbf{x}_s|\theta)\|^2 \right] + \frac{1}{N_s} \max_{\theta} \left[\frac{1}{N_s} \|\nabla \log p(\mathbf{x}_s|\theta)\|^2 + \sum_{x_i \in \mathbf{x}_s} \|\nabla \log p(x_i|\theta)\|^2 \right], \quad (5e)$$

in which only the first term depends on q_s .

F Additional experiments

In this section, we provide additional results for Bayesian linear regression. Since we can leverage the simple likelihood function and compute surrogates analytically, this setting is especially useful to understand the behavior of our method.

F.1 Linear regression

In this set of experiments, we apply CG-DSGLD to Bayesian linear regression and analyze its performance, which we measure in terms of MSE averaged over posterior samples.

Model The inputs of our model are $\mathbf{Z} = \{x_i, y_i\}_{i=1}^N$, where $x_i \in \mathbb{R}^d$ and $y_i \in \mathbb{R}$. The likelihood of the i th output $y_i \in \{0, 1\}$, given the input vector x_i , is $p(y_i|x_i) = \mathcal{N}(y_i|\beta^\top x_i, \sigma_e)$, and we place the prior $p(\beta) = \mathcal{N}(\beta|\mathbf{0}, \lambda^{-1}I)$.

Setting We run experiments on four different datasets⁴ from the UCI repository: Concrete (1030 samples, 9 features); Noise (1503 samples, 6 features); Conductivity (17389 samples, 81 features); and Localization (535004 samples, 386 features). We normalize and partition our datasets into (80%) training and (20%) test sets. In all our experiments, both DSGLD and CG-DSGLD have the same hyper-parameters. We sample $S = 10$ disjoint data subsets for $r = 1000$ rounds each having 600 iteration per round, with fixed step-size $h_t = 10^{-5}$ and mini-batch size $m = 10$. All shards are chosen with same probability $f_1 = \dots = f_S = 1/S$. We also burn-in the first ten thousand samples and thin the remaining by a hundred. We set $q_s(\theta) = \mathcal{N}(\theta|\mu, \Sigma)$, with $\Sigma = (\mathbf{x}^\top \mathbf{x})^{-1}$ and $\mu = (\sum y_i x_i) \Sigma^{-1}$, for each $s = 1 \dots S$. We repeated the same experiment for 10 different random seeds. We report the average test MSE and its variance as a function of the number of posterior samples.

Results Figure 6 shows the cumulative MSE and its variance. Overall, CG-DSGLD converges faster than DSGLD in MSE, with the notable exception of the Conductivity dataset, for which both methods converge virtually at the same time. In the case of the Noise dataset, CG-DSGLD additionally converges to a much lower MSE. Notably, our method also presents clearly lower variance for all datasets.

References

- Ahn, S., Shahbaba, B., and Welling, M. (2014). Distributed stochastic gradient MCMC. In *International Conference on Machine Learning (ICML)*.
- Chen, C., Ding, N., and Carin, L. (2015). On the convergence of stochastic gradient MCMC algorithms with high-order integrators. In *Advances in Neural Information Processing Systems (NeurIPS)*.
- Dubey, K. A., Reddi, S. J., Williamson, S. A., Póczos, B., Smola, A. J., and Xing, E. P. (2016). Variance reduction in stochastic gradient langevin dynamics. In *Advances in Neural Information Processing Systems (NeurIPS)*.

⁴Datasets can be downloaded from <https://archive.ics.uci.edu/ml/index.html>

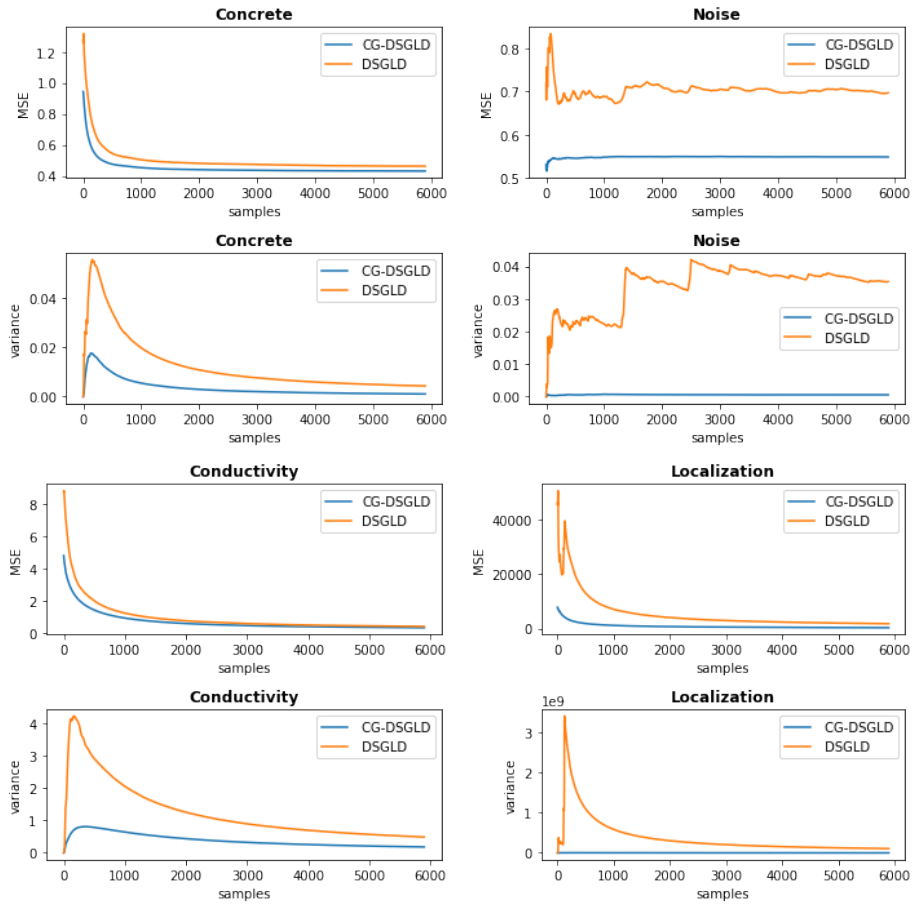


Figure 6: Average MSE and variance along time computed for DSGLD and CG-DSGLD as a function of the number of samples. Overall, CG-DSGLD converges to better performance than DSGLD. Additionally, CG-DSGLD shows lower variance for all datasets.